Organotin(IV) Derivatives of Some O,C,O-Chelating Ligands

Roman Jambor,*,† Libor Dostál,† Aleš Růžička,† Ivana Císařová,‡ Jiří Brus,§ Michal Holčapek,⊥ and Jaroslav Holeček†

Department of General and Inorganic Chemistry and Department of Analytical Chemistry, Faculty of Chemical Technology, University of Pardubice, nám. Čs. legií 565, CZ-532 10, Pardubice, Czech Republic, Faculty of Science, Charles University in Prague, Hlavova 2030, 128 40 Praha 2, Czech Republic, and Institute of Macromolecular Chemistry of the Academy of Sciences of the Czech Republic, Heyrovsky sq. 2, 162 06 Praha 6, Czech Republic

Received May 6, 2002

The series of organotin(IV) complexes $L^{1-3}SnPh_nCl_{3-n}$, where L^{1-3} are O,C,O-chelating ligands (called the pincer ligands), 2,6-bis(alkoxymethyl)phenyl-, 2,6-$(ROCH_2)_2C_6H_3^-$ (L^1, R = Me, L^2, R = *i*-Pr, L^3, R = *t*-Bu, $n = 3-0$), have been synthesized and characterized by ^1H, ^{13}C, and ^{119}Sn NMR spectroscopy, MS-ESI spectrometry, and elemental analysis. The structure of selected compounds L^1SnPh_3 (**1**), L^1SnPh_2Cl (**2**), $L^1SnPhCl_2$ (**3**), L^1SnCl_3 (**4**), $L^2SnPhCl_2$ (**7**), and $L^3SnPhCl_2$ (**11**) was studied by X-ray crystallography and ^{119}Sn CP/MAS NMR spectroscopy in the solid state. The determination of crystal structures reveals the similarity of all the shapes of coordination polyhedra. The deformations of the shapes of coordination polyhedra depend on the degree of donor−acceptor Sn−O interaction (from very weak (interatomic distance Sn−O 2.963(1) Å) to medium-strong (2.475(1) Å)), which increases with increasing Lewis acidity of the tin atom in the $L^{1-3}SnPh_nCl_{3-n}$ entities and decreases with increasing steric demands of substituents R (from Me to *t*-Bu). NMR spectroscopy indicates a similar structural arrangement of the studied compounds in solution.

Introduction

Investigation of the organotin compounds is interesting because of their biological activity,[1] reactivity,[2] and industrial applications.[3] Unexpected structural aspects and reactivities are usually associated with the presence of so-called hypervalent or hypercoordinated organotin compounds.[4] The representatives of such organotin compounds containing intramolecularly coordinating Y,C,Y-chelating ligands (Y = heteroatom-containing substituent) seem to be very popular at the present time. In particular, nitrogen-containing ligands of this Y,C,Y-type **A** (Chart 1) are studied extensively.

Chart 1

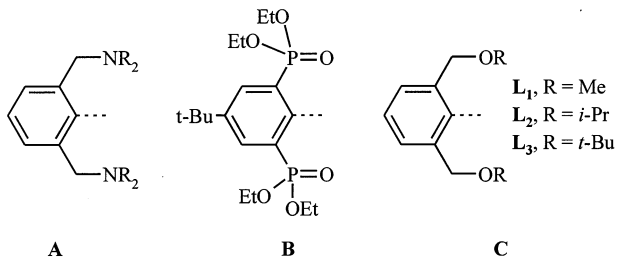

A **B** **C**

R = Me, Et, *i*-Pr, *t*-Bu

Recently, this nitrogen-containing type of ligand has been shown to be very useful in organotin cation stabilization.[5] On the other hand, only a few examples of oxygen donor atom-containing ligands of this Y,C,Y-type are known. Recently, Jurkschat et al. reported the synthesis of a series of organotin compounds containing an O,C,O-coordinating pincer ligand of type **B** (Chart 1), in which the possibility of hypercoordination of the tin atom through Sn−O interaction has been demonstrated.[6] On the basis of this information, we have decided to focus on synthesis of new O,C,O-chelating ligands of type **C** (Chart 1).

* Corresponding author. Fax: ++420 46 603 7068. E-mail: roman.jambor@upce.cz.
† Department of General and Inorganic Chemistry, University of Pardubice.
‡ Charles University in Prague.
§ Institute of Macromolecular Chemistry of the Academy of Sciences of the Czech Republic.
⊥ Department of Analytical Chemistry, University of Pardubice.

(1) (a) Nath, M.; Yadav, R.; Eng G.; Musingarimi, P. *Appl. Organomet. Chem.* **1999**, *13*, 29, and references therein. (b) Crowe, A. J. In *Metal Complexes in Cancer Chemotherapy*; Keppler, B. K., Ed.; VCH: Weinheim, Germany, 1993; pp 369−379. (c) Gielen, M.; Lelievield, P.; de Vos, D.; Willem, R. Metal-Based Drugs. In *Metal-Based Antitumor Drugs*; Gielen, M., Ed.; Freund Publishing House: Tel Aviv, Israel, 1992; Vol. 2, pp 29−54.

(2) (a) Pieper, N.; Klaus-Mrestani, C.; Schürmann, M.; Jurkschat, K.; Biesemans, M.; Verbruggen, I.; Martins, J. C.; Willem, R. *Organometallics* **1997**, *16*, 1043. (b) Kolb, U.; Dräger, M.; Dargatz, M.; Jurkschat, K. *Organommetallics* **1995**, *14*, 2827. (c) Dakternieks, D.; Dyson, G.; Jurkschat, K.; Tozer, R.; Tiekink, E. R. T. *J. Organomet. Chem.* **1993**, *458*, 29.

(3) Pinnavaia, T. J. *Science* **1983**, *220*, 4595.

(4) (a) Akiba, K., Ed. *Chemistry of Hypervalent Compounds*; Wiley-VCH: Weinheim, Germany, 1999, and references therein. (b) Jastrzebski, J. T. B. H.; Boersma, J.; Esch, P. M.; van Koten, G. *Organometallics* **1991**, *10*, 930. (c) Mitzel, N. W.; Losehand, U.; Richardson A. *Organometallics* **1999**, *18*, 2610. (d) Buntine, M. A.; Kosovel, F. J.; Tiekink, R. T. *Phosphorus, Sulfur Silicon Relat. Elem.* **1999**, *150−151*, 261, and references therein. (e) Jurkschat, K.; Pieper, N.; Seemeyer, S.; Schürmann, M.; Biesemans, M.; Verbruggen, I.; Willem, R. *Organometallics* **2001**, *20*, 868.

(5) (a) Jambor, R.; Císařová, I.; Růžička, A.; Holeček, J. *Acta Crystallogr.* **2001**, *C57*, 373. (b) van Koten, G.; Noltes, J. G. *J. Am. Chem. Soc.* **1976**, *98*, 5393.

10.1021/om020361i CCC: $22.00
Publication on Web 08/23/2002

Scheme 1

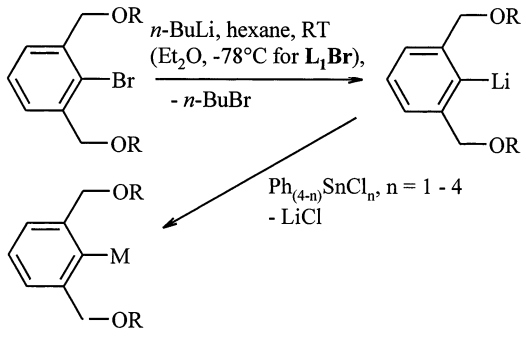

1, R = Me, M = $SnPh_3$
2, R = Me, M = $SnPh_2Cl$
3, R = Me, M = $SnPhCl_2$
4, R = Me, M = $SnCl_3$
5, R = *i*-Pr, M = $SnPh_3$
6, R = *i*-Pr, M = $SnPh_2Cl$
7, R = *i*-Pr, M = $SnPhCl_2$
8, R = *i*-Pr, M = $SnCl_3$
9, R = *t*-Bu, M = $SnPh_3$
10, R = *t*-Bu, M = $SnPh_2Cl$
11, R = *t*-Bu, M = $SnPhCl_2$

This paper describes the synthesis of monoanionic O,C,O-chelating ligands $[C_6H_3(CH_2OR)_2\text{-}2,6]^-$ (R = Me (L^1), *i*-Pr (L^2), and *t*-Bu (L^3)) and their organotin derivatives (**1**−**11**) (Scheme 1).

Detailed solution NMR studies of these compounds and also solid state NMR studies and X-ray crystal structure determinations of selected compounds **1**−**4**, **7**, and **11** are described. These compounds enable study of the effect of moderation of the Lewis acidity of the tin center on the number and magnitude of the intramolecular tin−oxygen interactions (**1**−**4**). Furthermore, this series also enables us to observe the dependence of the Sn−O interaction strength on increasing ligand spatial hindrance (**3**, **7**, **11**).

Results and Discussion

Synthetic Aspects. The 1-bromo-2,6-bis(alkoxymethyl)benzenes ($L^{1-3}Br$) were used as starting compounds to prepare all of compounds **1**−**11**. The reaction of 1-bromo-2,6-bis(bromomethyl)benzene with excess sodium methanolate or potassium *tert*-butoxyde affords 1-bromo-2,6-bis(methoxymethyl)benzene (L^1Br) and 1-bromo-2,6-bis(*tert*-butoxymethyl)benzene (L^3Br) with good yields (eq 1), while the isopropoxy-substituted

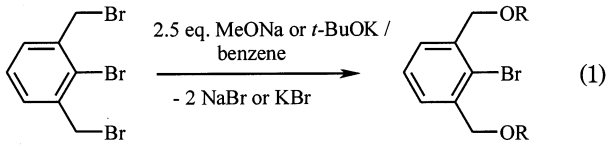

(1)

R = Me, **L^1Br**
R = *t*-Bu, **L^3Br**

ligand (L^2Br) was prepared by the reaction of 1-bromo-2,6-bis(bromomethyl)benzene with 2-propanol in the presence of excess of AgO (eq 2). This way of preparation led to higher yield of this compound.

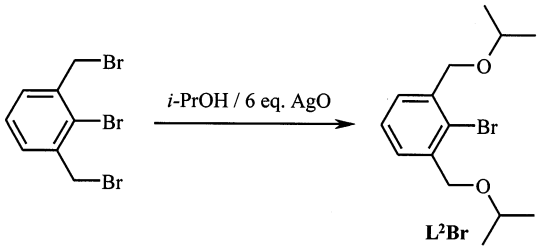

(2)

Compounds **1**−**4** were prepared as white crystalline solids by reaction of L^1Br with *n*-BuLi followed by addition to a precooled hexane solution of the appropriate organotin halide. If both the solutions (Li salt and organotin halide) are prepared in Et_2O/hexane at −78 °C, the best yield is obtained (no attack of the solvent was observed at this temperature),[7] while at 0 °C L^1Li metalates Et_2O, and consequently no formation of compounds **1**−**4** was observed at this temperature. Treatment of L^2Br (L^3Br) with *n*-BuLi in hexane at ambient temperature results in a yellow solution, from which the L^2Li (L^3Li) salt is obtained as a white solid, following crystalization from the saturated hexane solution at −78 °C. The subsequent reaction of the L^2Li (L^3Li) salt with the appropriate organotin halide led to formation of compounds **5**−**8** (**9**−**11**) (see Scheme 1).

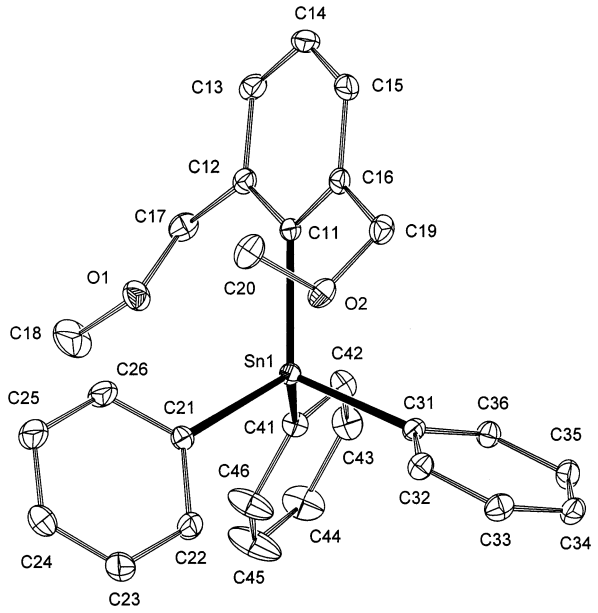

Figure 1. General view (ORTEP) of a molecule showing 30% probability displacement ellipsoids and the atom-numbering scheme for **1**. The hydrogen atoms are omitted for clarity.

Molecular Structures of 1−4, 7, and 11. The molecular structures of these compounds are depicted in Figures 1−6, respectively. The crystallographical data and selected bond lengths and angles are given in Tables 1−2.

The shapes of the coordination polyhedra are mutually similar for all the studied compounds. They differ from tetrahedral arrangement only in the extent of

(6) (a) Mehring, M.; Vrasidas, I.; Horn, D.; Schürmann, M.; Jurkschat, K. *Organometallics* **2001**, *20*, 4647. (b) Mehring, M.; Löw, Ch.; Uhlig, F.; Schürmann, M.; Jurkschat, K.; Mahieu, B. *Organometallics* **2000**, *19*, 4613. (c) Vicente, J.; Arcas, A.; Blasco, M. A.; Lozano, J.; de Arellano, M. C. R. *Organometallics* **1998**, *17*, 5374.

(7) For similar results see: Dakternieks, D.; Jurkschat, K.; Tozer, R.; Hook, J.; Tiekink, E. R. T. *Organometallics* **1997**, *16*, 3696.

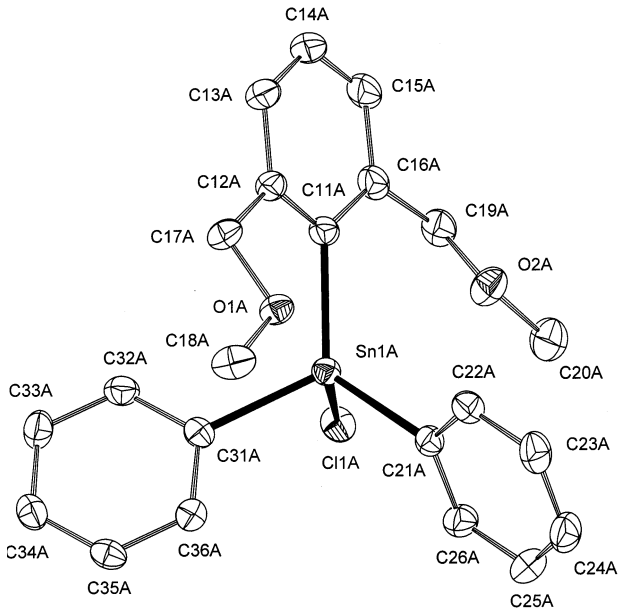

Figure 2. General view (ORTEP) of a molecule showing 50% probability displacement ellipsoids and the atom-numbering scheme for **2**. Only one molecule from the crystal lattice of **2** without hydrogen atoms has been chosen for clarity.

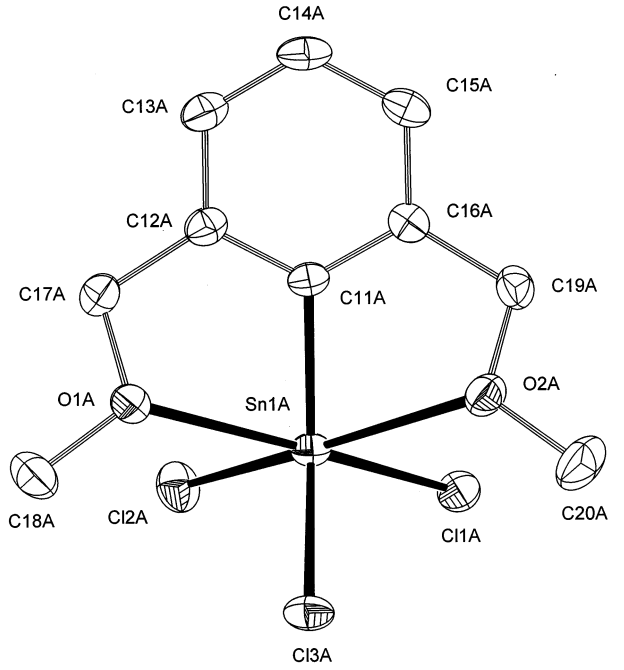

Figure 4. General view (ORTEP) of a molecule showing 50% probability displacement ellipsoids and the atom-numbering scheme for **4**. Only one molecule from the crystal lattice of **4** without hydrogen atoms has been chosen for clarity.

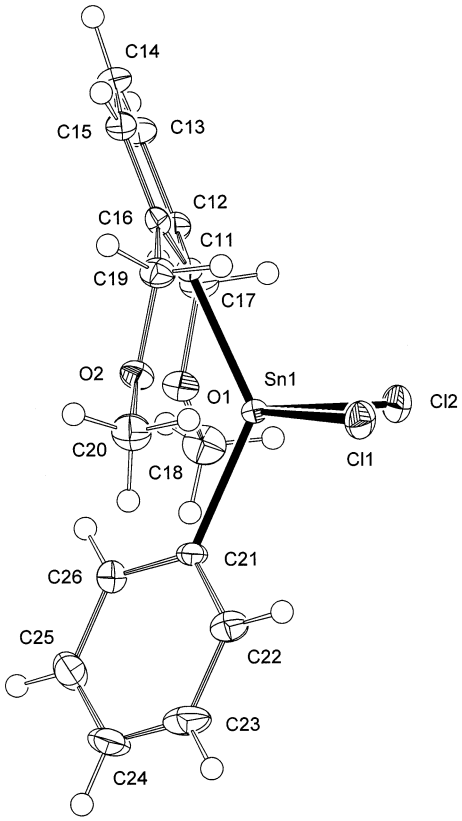

Figure 3. General view (ORTEP) of a molecule showing 50% probability displacement ellipsoids and the atom-numbering scheme for **3**.

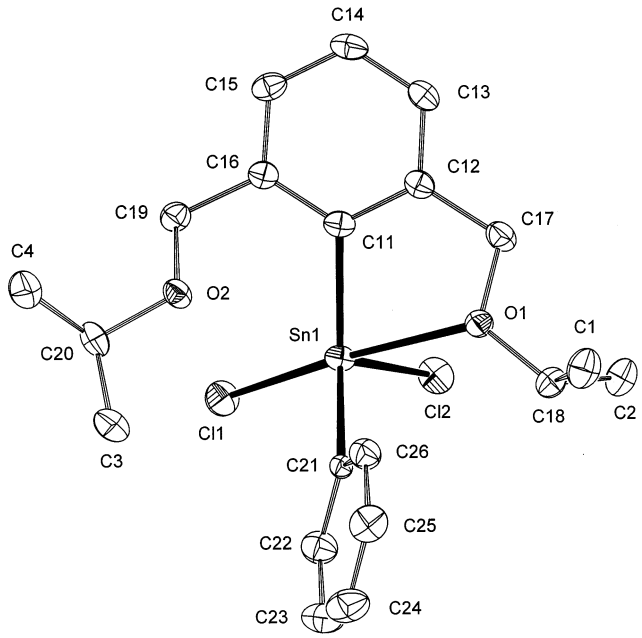

Figure 5. General view (ORTEP) of a molecule showing 50% probability displacement ellipsoids and the atom-numbering scheme for **7**. The hydrogen atoms are omitted for clarity.

declinations, resulting in a natural transformation of the tetrahedron to an octahedron on passage from **1** to **4**.[8] The values of Sn−O bond lengths (from 2.475(1) to 2.966(1) Å) are substantially smaller than the sum of the van der Waals radii of oxygen and tin (3.70 Å)[9] in the studied compounds, but larger than the sum of the covalent radii (2.066 Å),[9] thus representing a weak or medium-strong Sn−O interaction. As a consequence of this interaction, some carbon and chlorine atoms depart

(8) The other interpretation of selected crystal structures can be that compounds **1** and **11** are examples of [4+2] coordination where a C_4Sn- (for **1**) and C_2Cl_2Sn- (for **11**) tetrahedron is *cis*-attacked by two oxygen donor atoms, while compounds **2** and **7** are examples of [5+1] coordination where distorted C_3ClOSn-trigonal bipyramids are attacked by an oxygen donor atom.

(9) Bondi, A. *J. Phys. Chem.* **1964**, *68*, 441.

Table 1. Crystallographic Data for 1−4, 7, and 11

	1	2	3	4	7	11
formula	$C_{28}H_{28}O_2Sn$	$C_{22}H_{23}ClO_2Sn$	$C_{16}H_{18}Cl_2O_2Sn$	$C_{10}H_{13}Cl_3O_2Sn$	$C_{20}H_{26}Cl_2O_2Sn$	$C_{23}H_{31}Cl_5O_2Sn$
MW	515.19	473.54	431.89	390.24	488.0	635.42
cryst syst	monoclinic	orthorhombic	trigonal	triclinic	monoclinic	orthorhombic
space group	$P2_1/n$ [No. 14]	*Pccn* [No. 56]	$P3_2$ [No. 145]	$P\bar{1}$ [No. 2]	$P2_1/n$ [No. 14]	$Pca2_1$ [No. 29]
a [Å]	13.9090(2)	24.9610(1)	12.5240(2)	9.5510(3)	13.4890(3)	17.8700(2)
b [Å]	12.3270(10)	25.6590(2)	12.5240(2)	12.1790(3)	8.6040(2)	13.4180(2)
c [Å]	14.6260(2)	12.8190(2)	9.2900(2)	12.6470(4)	17.7460(3)	11.3790(2)
α [deg]				106.9140(18)		
β [deg]	106.5671(7)			99.2940(16)	97.8520(13)	
γ [deg]			120.00	94.0710(19)		
Z	4	16	3	4	4	4
V [Å^3]	2403.61(5)	8210.24(15)	1261.92(4)	1378.12(7)	2040.28(7)	2728.45(7)
D_x [g cm^{-3}]	1.424	1.532	1.705	1.881	1.589	1.547
cryst size [mm]	0.3 × 0.27 × 0.12	0.48 × 0.12 × 0.1	0.5 × 0.5 × 0.35	0.25 × 0.25 × 0.12	0.25 × 0.15 × 0.075	0.3 × 0.2 × 0.15
cryst shape	plate	bar	prism	plate	plate	bar
μ [mm^{-1}]	1.084	1.388	1.837	2.418	1.525	1.444
θ_{max} [deg]	27.50	27.50	29.13	27.54	27.50	27.50
range of *h*;*k*;*l*	−18,18; 15,16; −19,18	−32,32; −33,33; −16,16	−17,17; −17,17; −12,12	−10,12; −15,15; −16,15	−17,17; −11,11; −22,23	−21,23;−17,17; −14,14
no. of measd reflns	43 076	124 846	16 486	23 056	32 616	45 202
no. of ind diffract. (R_{int}[a])	5504 (0.040)	9420 (0.054)	4497 (0.031)	6251 (0.045)	4684 (0.044)	6257 (0.043)
no. of obsd diffract. [$I > 2\sigma(I)$]	5005	7696	4452	5903	4115	5772
T_{min}, T_{max}	0.804, 0.899	0.801, 0.874	0.508,0.583	0.561, 0.740	0.798,0.895	0.696, 0.810
no. of params	282	473	192	293	230	286
w_1, w_2[b]	0.0261, 1.3408	0.0373, 6.9015	0.076,0.2685	0.0242, 1.6462	0.0293,1.1498	0.0400, 1.4556
abs struct param (Flack)			−0.012(10)			−0.015(17)
R,[c] *wR* for obsd diffract.	0.022, 0.054	0.029, 0.070	0.015,0.034	0.026, 0.067	0.026, 0.059	0.028,0.069
R; w*R* for all data	0.026,0.056	0.041, 0.076	0.015,0.034	0.028, 0.068	0.033, 0.062	0.032, 0.071
GOF[d]	1.052	1.055	1.112	1.093	1.046	1.049
residual electron density [e/Å^3]	0.382, −0.783	0.658, −0.761	0.306, −0.504	0.953, −0.924	0.743, −0.839	0.715, −0.542

[a] $R_{int} = \Sigma|F_o^2 - F_{o,mean}^2|/\Sigma F_o^2$. [b] Weighting scheme: $w = [\sigma^2(F_o^2) + (w_1P)^2 + w_2P]^{-1}$, where $P = [\max(F_o^2) + 2F_c^2]$. [c] $R(F) = \Sigma||F_o| - |F_c||/\Sigma|F_o|$, $wR(F^2) = [\Sigma(w(F_o^2 - F_c^2)^2)/(\Sigma w(F_o^2)^2)]^{1/2}$. [d] GOF $= [\Sigma(w(F_o^2 - F_c^2)^2)/(N_{diffrs} - N_{params})]^{1/2}$.

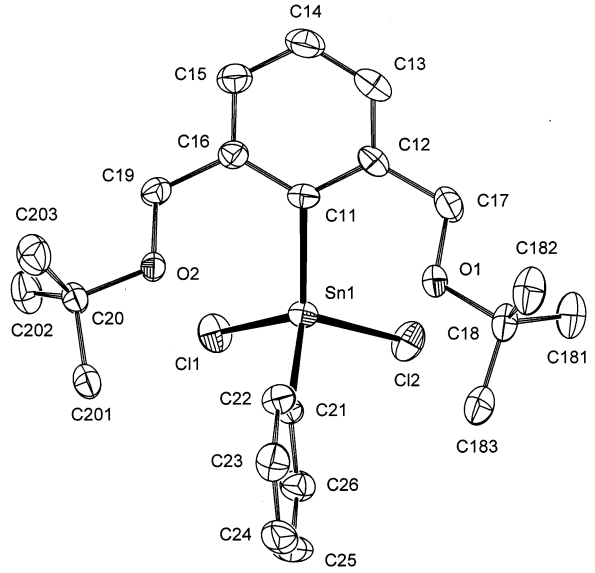

Figure 6. General view (ORTEP) of a molecule showing 50% probability displacement ellipsoids and the atom-numbering scheme for **11**. The hydrogen atoms and molecule of $CHCl_3$ are omitted for clarity.

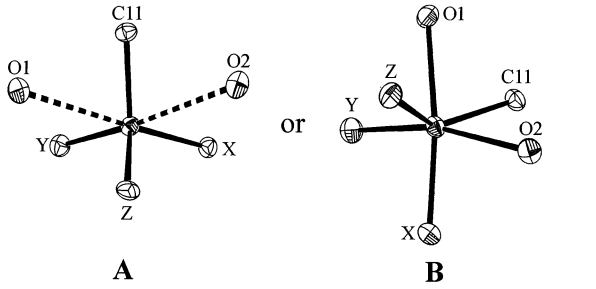

Figure 7. Alternative descriptions of coordination geometry (tetrahedron **A**, octahedron **B**) of the studied compounds.

from true tetrahedral geometry, being situated in the *pseudotrans* positions in relation to both oxygen atom (see the values of angles O(1)−Sn−X and O(2)−Sn−Y in Table 2).

Together with the central tin atoms, these atoms form the equatorial plane of a deformed octahedron in another description of the coordination geometry of the studied compounds. The other atoms bonded to the tin atom occupy the axial positions (Figure 7). The oxygen donor groups are bound to the tin atom in *cis* fashion, resulting in a *pseudofacial* O,C,O-coordination mode of the "pincer" ligands in this description. This *cis* arrangement of oxygen atoms is retained even in diorganotin compounds **3**, **7**, and **11**, in contrast to the related diorganotin dichloride derivatives containing another O,C,O-coordinating pincer ligand, $C_6H_2[P(O)(OEt)_2]_2$-1,3-*t*-Bu-5, where the oxygens are bound to the tin atom in *trans* fashion.[10]

As the average C−Sn−C angle is 109.22° (109.56° in the unsubstituted Ph_4Sn analogue[11]), the geometry of

(10) Mehring, M.; Schürmann, M.; Jurkschat, K. *Organometallics* **1998,** *17*, 1227.

Table 2. Selected Bond Distances (Å) and Angles (deg) Found in Selected Compounds 1−4, 7, and 11

	1 X=C31, Y=C41, Z=C21	**2A** X=Cl1A, Y=C31A, Z=C21A	**2B** X=Cl1B, Y=C31B, Z=C21B	**3** X=Cl1, Y=Cl2, Z=C21	**7** X=Cl1, Y=Cl2, Z=C21	**11** X=Cl1, Y=Cl2, Z=C21	**4A** X=Cl1A, Y=Cl2A, Z=Cl3A	**4B** X=Cl1B, Y=Cl2B, Z=C13B
Sn1−C11	2.165(2)	2.136(2)	2.138(2)	2.117(1)	2.126(2)	2.132(3)	2.103(2)	2.110(2)
Sn1−O1	2.908(1)	2.567(2)	2.586(2)	2.619(1)	2.475(1)	2.775(2)	2.511(2)	2.513(2)
Sn1−O2	2.966(1)	2.993(2)	2.891(2)	2.655(1)	2.985(2)	2.882(2)	2.557(2)	2.583(2)
Sn1−X	2.168(2)	2.457(1)	2.440(1)	2.395(1)	2.401(1)	2.388(1)	2.383(1)	2.383(1)
Sn1−Y	2.153(2)	2.137(2)	2.148(2)	2.398(1)	2.378(1)	2.376(1)	2.391(1)	2.365(1)
Sn1−Z	2.144(2)	2.125(2)	2.130(2)	2.121(2)	2.142(2)	2.112(3)	2.340(1)	2.337(1)
C11−Sn1−X	112.85(6)	105.95(7)	104.49(7)	110.54(5)	112.26(6)	100.78(8)	111.81(7)	109.88(7)
C11−Sn1−Y	109.36(6)	114.86(9)	113.42(9)	105.26(4)	106.53(6)	111.57(8)	110.47(7)	117.02(7)
C11−Sn1−Z	116.98(6)	121.91(9)	123.93(9)	131.30(6)	129.13(8)	125.4(1)	132.62(7)	127.95(7)
C11−Sn1−O1	65.56(5)	71.07(8)	70.26(7)	70.08)5)	72.41(7)	69.08(9)	70.07(8)	69.86(8)
C11−Sn1−O2	66.81(5)	64.15(7)	64.94(7)	68.28(5)	64.82(6)	68.00(9)	68.80(8)	69.04(8)
O1−Sn1−O2	112.01(4)	114.42(5)	113.12(6)	116.95(4)	118.43(4)	118.83(6)	113.75(6)	114.89(6)
O1−Sn1−X	172.55(5)	166.79(4)	166.44(4)	165.09(3)	168.69(4)	162.91(5)	168.42(5)	165.90(5)
O1−Sn1−Y	74.71(5)	78.43(7)	77.59(7)	76.68(3)	79.66(4)	75.60(5)	79.08(5)	78.20(4)
O1−Sn1−Z	79.67(5)	89.18(7)	89.25(8)	87.13(6)	83.56(6)	85.78(9)	85.54(5)	86.25(5)
O2−Sn1−X	72.76(5)	74.01(4)	73.96(5)	75.70(3)	72.44(3)	74.86(5)	76.90(5)	76.91(5)
O2−Sn1−Y	168.05(5)	164.12(7)	166.15(8)	159.19(3)	152.85(3)	162.00(5)	164.70(5)	166.85(5)
O2−Sn1−Z	81.78(5)	77.41(7)	78.09(8)	86.75(5)	90.76(6)	85.72(9)	86.40(5)	81.69(4)
X−Sn1−Y	99.61(6)	91.74(6)	93.81(6)	89.03(2)	89.07(2)	89.16(3)	89.73(2)	89.95(2)
X−Sn1−Z	107.04(6)	102.92(7)	103.78(7)	102.07(5)	100.03(5)	106.41(8)	100.12(2)	103.72(2)
Y−Sn1−Z	109.58(6)	113.38(9)	111.80(9)	110.58(4)	112.40(5)	107.11(9)	103.49(3)	101.24(2)

1 is nearly tetrahedral. The greatest deviations from ideal tetrahedral shape are found for C(11)−Sn−C(21) and C(31)−Sn−C(41), 117.11° and 99.33°, respectively (in Ph_4Sn 108.6° and 111.2°).[11] The values of both Sn−O bonds (2.909 and 2.963 Å, respectively) indicate relatively weak intramolecular interactions, but stronger than those in another triphenyltin(IV) compound containing another O,C,O-pincer ligand, $C_6H_2[P(O)(OEt)_2]_2$-1,3-*t*-Bu-5 (3.006 and 3.022 Å, respectively).[10] The Sn−C(21) bond distance is almost identical with the average bond distance in Ph_4Sn, while the other Sn−C bonds are slightly longer. The elongation of the Sn−C(11) bond is caused by steric repulsion of the relative rigid "pincer" ligand,[12] and that of Sn−C(31) and Sn−C(41) is a consequence of their location in *pseudotrans* positions with respect to the oxygen atoms.[13]

The stepwise shortening of the Sn−O bond distances from **1** to **4** (increasing Lewis acidity of central tin atoms) indicates an increasing degree of Sn−O donor−acceptor interaction. The slight forcing of the Sn−O coordination leads to a shift in the real shape of the coordination polyhedron toward octahedral in the tetrahedron−octahedron path. The distortion from tetrahedral geometry is correlated with the magnitude of the Sn−O interaction (see Table 2) and is documented by increasing values of the axial angles defined as C(11)−Sn−C(21) (compounds **1**−**3**) and C(11)−Sn−Cl(3) (compound **4**), respectively (Figure 7A, B). The Sn−C and Sn−Cl distances are also slightly shortened stepwise, due to forcing of the Sn−O donor−acceptor interaction.

The coordination geometries of **3**, **7**, and **11** (Figures 3, 5, and 6) seem to be strongly influenced by steric factors. Despite the slight increase in the Lewis basicity of the oxygen donor centers in the CH_2OR groups in this set, the Sn−O donor−acceptor interaction is weakened stepwise (see Table 2), as a consequence of steric repulsion forces of R groups in the CH_2OR substituents, which predominates over the effect of the Sn−O donor−acceptor interaction.

Table 3. Selected ^{13}C and ^{119}Sn NMR Data[a] for 1−11

compd	$\delta(^{119}Sn)_{iso}$ [ppm][b]	$\delta(^{119}Sn)$ [ppm]	$\delta(^{13}C(1))$ [ppm][c] ($^nJ(^{119}Sn, ^{13}C(1))$ [Hz])	$\delta(^{13}C(1'))$ [ppm][d] ($^nJ(^{119}Sn, ^{13}C(1'))$ [Hz])
1	−163.2	−163.3	137.2 (570.8)	142.5 (543.1)
2	−155.2	−144.4	135.3 (729.6)	142.4 (733.9)
	−163.3			
3	−196.5	−208.8	134. 8 (997.4)	141.2 (1027.2)
4	−236[e]	−270.5	138.7 (1372.2)	
5		−153.8	135.5 (542.4)	141.5 (527.1)
6		−136.1	134.2 (683.8)	143.2 (737.9)
7	−191.9	−177.4	132.9 (930.5)	143.4 (996.1)
8		−238.8	139.6 (1036.2)	
9		−154.0	133.6 (536.1)	141.4 (520.9)
10		−121.7	134.2 (714.4)	143.3 (720.6)
11	−161.5	−148.5	132.1 (872.4)	144.6 (945.9)

[a] Measured in $CDCl_3$. [b] ^{119}Sn CP/MAS was measured only for selected compounds **1**−**4**, **7**, and **11**. [c] Refers to the tin-bound *ipso*-carbon of the O,C,O-pincer ligand. [d] Refers to the tin-bound carbon of the phenyl groups. [e] Broad signal.

The existence of one independent molecule in the crystal lattice of the studied compounds (except **2** and **4**, mentioned above) is also reflected by the observation of only one ^{119}Sn CP/MAS NMR resonance. In addition, the values of $\delta(^{119}Sn)_{iso}$ are close to the values of the ^{119}Sn NMR shifts in solution (see Table 3), indicating that no intermolecular coordination is present in the solid state in the studied compounds. The observation of two resonances in the ^{119}Sn CP/MAS NMR spectrum for **2** (−155.2 and −163.3 ppm) is in agreement with the presence of two independent molecules in the crystal lattice of **2**, while the same result has not been found because of the very broad signal (probably due to the presence of three quadrupolar atoms $^{35,37}Cl$ in the molecule) in the ^{119}Sn CP/MAS NMR spectrum for **4**. The central signal patterns of the ^{119}Sn CP/MAS NMR spectra of the studied compounds (**2**, **3**, **7**, and **11**) are typical for organotin compounds, in which the tin atom is bonded to one or two chlorides.[14]

(11) Belsky, V. K.; Simonenko, A. A.; Reikhsfeld, V. O.; Saratov, I. E. *J. Organomet. Chem.* **1983**, *244*, 125.
(12) Vij, A.; Kirchmeier, R. L.; Willet, R. D.; Shreeve, J. M. *Inorg. Chem.* **1994**, *33*, 5456.
(13) Jastrzebski, J. T. B. H.; van Koten, G. *Adv. Organomet. Chem.* **1993**, *35*, 241.

Table 4. Temperature Dependence of Selected ^{1}H and ^{119}Sn NMR Parameters (range 170−300 K, Toluene-d_8)

compound	*T*, K	$\delta(^{119}Sn)^a$ [ppm]	$\delta(^1H)^a$ [ppm]	
			CH_2	CH_3
1	300	−162.3	4.09	2.58
	170	−161.1	3.92	2.48
2	300	−142.8	4.25	2.71
	170	−149.6	4.48/3.51	3.07/2.18
3	300	−201.3	4.29	2.88
	170	−215.8	4.61/3.31[b]	2.81
4	300	−268.1	4.02	3.17
	170	−285.2	*c*	3.13
5	300	−153.8	4.37	0.75[d]
	170	−152.0	4.24	0.74
6	300	−128.3	4.55	0.69[d]
	170	−152.0	4.94/3.83	0.92/0.12
7	300	−167.6	4.49	0.73[d]
	170	−184.3	4.70/3.93[e]	0.72/0.51[e]
8	300	−189.9	4.84	0.94[d]
	170	−193.4	*c*	1.01
9	300	−153.2	4.38	0.84
	170	−154.2	4.43	0.87
10	300	−115.2	4.62	0.85
	170	−133.2	5.07/4.20	0.95
11	300	−138.5	4.46	0.79
	170	−154.5	5.00/3.88[b]	0.94

[a] Measured in toluene-d_8. [b] AX pattern ($^2J_{H,H}$ = 11.8 Hz for **3** and 11.3 Hz for **11**). [c] Not observed. [d] Doublet. [e] Broad signal.

Solution NMR Study. The ^{119}Sn NMR shifts and $^1J(^{119}Sn,^{13}C)$ coupling constants were shown to be very sensitive indicators for elucidation of the coordination numbers and geometries of organotin compounds.[15] None of the compounds studied exhibited any concentration dependences of the ^{119}Sn NMR shifts, from which it is clear that no intermolecular interactions are present.

In tetraorganotin compounds **1**, **5**, and **9**, a four-coordinated tin atom without any or with very weak Sn−O interaction is indicated by the values of $\delta(^{119}Sn)$ and particularly by the values of the $^1J(^{119}Sn,^{13}C(1))$ and $^1J(^{119}Sn,^{13}C(1'))$ coupling constants (see Table 3), which differ only slightly from those for nonfunctional Ph_4Sn (−128.1 ppm, 531 Hz).[15a] The coordination geometry of the central tin atom is a slightly distorted tetrahedron, with bonding angles C(1)−Sn−C(1′) and C(1′)−Sn−C(1′) of approximately 109°, 107° for **1**; 107°, 106° for **5**, and 107°, 106° for **9**.[15c] Neither ^{1}H NMR nor ^{119}Sn NMR exhibits any important temperature dependences in the range studied (170−360 K, toluene-d_8, see Table 4).

In compounds **2**, **6**, and **10**, the values of $\delta(^{119}Sn)$ (see Table 3) (compare with −44.7 ppm for Ph_3SnCl)[15a] result in a higher coordination number for the tin atom than four. The existence of a weak Sn−O interaction is reflected in an increase in the values of the $^1J(^{119}Sn,13C(1))$ and $^1J(^{119}Sn,^{13}C(1'))$ coupling constants (614.3 Hz for Ph_3SnCl).[15a] The magnitudes of the calculated bonding angles C(1)−Sn−C(1′) and C(1′)−Sn−C(1′)[15c] (119°, 119° (**2**); 116°, 119° (**6**); and 118°, 118° (**10**)) indicate similar structures as in the solid state (see Figure 2 and Table 2). The $\delta(^{119}Sn)$ values are shifted upfield with decreasing temperature (170−360 K, toluene-d_8, see Table 4), thus indicating forcing of the Sn−O interaction at a lower temperature in these compounds. The dynamic behavior of **2**, **6**, and **10** with two *ortho*-CH_2OR substituents with different R groups was studied at various temperatures of ^{1}H NMR (170−360 K, toluene-d_8). At room temperature, the ^{1}H NMR spectrum displays one set of sharp signals for all the protons. As the temperature is decreased, first a broadening of the CH_2 (for **2**, **6**, and **10**), CH (for **6**), and CH_3 (for **2**, **6**, and **10**) protons is observed, followed by decoalescence of all the protons at 200 K for **2**, 185 K for **6**, and 170 K for **10**, which indicates, as is well-known, a dissociation/association dynamic procedure[16] in these compounds. The energy barriers ($\Delta G^{\ddagger}$) of the fluxional processes (calculated from the Eyring equation)[17] are 35.9 kJ mol^{-1} for **2**, 32.9 kJ mol^{-1} for **6**, and 30.4 kJ mol^{-1} for **10**. The explanation for observations of different decoalescence temperatures for **2**, **6**, and **10** can lie in the different strengths of the Sn−O interaction in these compounds in solution. The strongest Sn−O interaction seems to be in **2** (where R is Me), while an increase in the substituent steric bulk attenuates Sn−O coordination.

For compounds **3**, **7**, and **11**, the values of $\delta(^{119}Sn)$ (Table 3) correspond to the five or better [4+2] coordinated diphenyltin(IV) compounds (compare with −26.7 ppm for Ph_2SnCl_2).[15b] Further forcing of the Sn−O coordination is reflected in increasing of values $^1J(^{119}Sn,^{13}C(1))$ and $^1J(^{119}Sn,^{13}C(1'))$ (−786.0 Hz for Ph_2SnCl_2).[15b] The calculated bonding angle C(1)−Sn−C(1′) (136° (**3**), 133° (**7**), 130° (**11**)) permits the prediction that the shape of the tin atom coordination polyhedra going from the solid state is probably retained in solution (compare with the bonding angles in the crystal structures of these compounds). A ^{119}Sn NMR study of these compounds (temperature range 170−360 K) yielded parallel results to those obtained previously. The dynamic behavior of **3**, **7**, and **11** has been studied by variable-temperature ^{1}H NMR (170−360 K, toluene-d_8). At room temperature, the ^{1}H NMR spectrum again displays sharp signals for all protons. When the temperature is decreased, initially a broadeaning of the CH_2 signal (for **3**, **11**) is observed, continuing in decoalescence of the benzylic protons at 235 K for **3** and 190 K for **11**. These are visible as a sharp AX pattern, whereas the signals of OR groups are seen as an unresolved signal (singlet for Me in **3** and for *t*-Bu in **11**). The ^{1}H NMR data of these compounds under decoalescence temperatures (235 K for **3** and 180 K for **11**) can be explained only by the geometry A (Scheme 2), which is similar to those found in the solid state, with the two $-CH_2OR$ units being equivalent. In each $-CH_2OR$ unit, the benzylic protons are diastereotopic and can be seen as an AX pattern. When the temperature is raised, the benzylic protons become equivalent by Sn−O bond dissociation followed by rotation about the C−C bond (see B in Scheme 2). The activation energy for this

(14) Harris, R. K.; Sebald, A.; Furlani, D.; Tagliavini, G. *Organometallics* **1988**, *7*, 388.

(15) (a) Holeček, J.; Nádvorník, M.; Handlíř, K.; Lyčka, A. *J. Organomet. Chem.* **1983**, *241*, 177. (b) Holeček, J.; Nádvorník, M.; Handlíř, K.; Lyčka, A. *Collect. Czech. Chem. Commun.* **1990**, *55*, 1193. (c) Holeček, J.; Nádvorník, M.; Handlíř, K.; Lyčka, A. *Z. Chem.* **1990**, *30*, 265. (d) Lyčka, A.; Holeček, J.; Schneider, B.; Straka, J. *J. Organomet. Chem.* **1990**, *389*, 29. (e) Pejchal, V.; Holeček, J.; Lyčka, A. *Sci. Univ. Pap. Pardubice* **1996**, *A2*, 35; *Chem. Abstr.* **1997**, *126*, 317445.

(16) Handwerker, H.; Leis, C.; Probst, R.; Bassinger, P.; Grohmann, A.; Kiprof, P.; Herdtweek, F.; Blümel, J.; Auner, N.; Zybill, C. *Organometallics* **1993**, *12*, 2162.

(17) Eyring equation: $\Delta G^{\ddagger} = -RT_c \ln[2\pi h(\Delta\nu)/kT\sqrt{3}]$ with $\Delta G^{\ddagger}$ = free energy of activation (J), T_c = coalescence temperature (K), and $\Delta\nu$ = chemical shift difference (Hz); the other symbols have their usual meanings.

Scheme 2

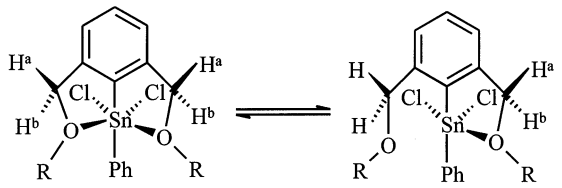

process is $\Delta G^{\ddagger} = 41.9$ kJ mol^{-1} for **3** and 31.9 kJ mol^{-1} for **11**. Both the alkyl groups appear as one signal because of the very fast rotation around the benzylic carbon−oxygen axis.

The dynamic study of **7** has resulted in a different dynamic process. When the temperature is decreased, initially broadening of the C*H*$_2$, C*H*, and C*H*$_3$ signals is observed, continuing in their decoalescence at 210 K, and two rather broad signals for C*H*$_2$, C*H*, and C*H*$_3$ protons can be seen in **7**. This dynamic process (similar to that in compounds **2**, **6**, and **10**) involves exchange between the coordinated and noncoordinated ether groups in **7** ($\Delta G^{\ddagger} = 38.0$ kJ mol^{-1}). The observation of different decoalescence temperatures for **3**, **7**, and **11** can be explained in the same way as in the previous case.

Monoorganotin compounds **4** and **8** contain a [4+2] coordinated tin atom, due to a relatively strong Sn−O interaction ($\delta(^{119}\text{Sn}) = -270.5$ (**4**) and −238.8 ppm (**8**), $^1J(^{119}\text{Sn},^{13}\text{C}(1)) = 1372.2$ (**4**) and 1036.2 (**8**) Hz, in $CDCl_3$) (−61.3 ppm and 1121.2 Hz for $PhSnCl_3$).[15e] The ^{119}Sn NMR shifts do not exhibit any temperature dependence in the range studied (170−360 K in toluene-d_8), and the dynamic behavior of these compounds, studied with variable-temperature ^{1}H NMR (170−360 K, toluene-d_8), exhibits a broadening of the C*H*$_2$ signals, but no signals were observed in the range 220−170 K.

Conclusion

Eleven original organotin(IV) derivatives of a novel type of oxygen-containing pincer ligand have been prepared, and the structures were estimated in solution and in the solid state for selected compounds. The existence of an Sn−O coordination bond has been proven using the NMR spectral parameters. The relation of the strength of the Sn−O interaction to different bulkiness of the ligands is evident in the values of $\delta(^{119}\text{Sn})$, of the coupling constants in solution, and of the Sn−O bond lengths. Different temperatures of decoalescence (CH_2 signals in the ^{1}H NMR spectrum) are also proof of variable strength of the Sn−O interaction. Determination of the crystal structures reveals the similarity of the shapes of coordination polyhedra, differing mutually from ideal arrangement only in the extent of the declinations. In all crystal structures, the oxygen donor groups are bound to the tin atom in *cis* fashion, resulting in a *pseudofacial* O,C,O-coordination mode of the "pincer" ligands.

Experimental Section

General Methods. Solvents were dried by standard methods and distilled prior to use. All moisture- and air-sensitive reactions were carried out under an argon atmosphere using standard Schlenk techniques.

The ^{119}Sn, ^{13}C, and ^{1}H NMR spectra were acquired on Bruker AMX360 or Avance500 spectrometers at 300 K in $CDCl_3$ or in toluene-d_8 (range 360−170 K). Appropriate chemical shifts were calibrated on the ^{1}H-residual peak of $CHCl_3$ ($\delta = 7.25$ ppm) or toluene ($\delta = 2.09$ ppm), the ^{13}C residual peak of $CHCl_3$ ($\delta = 77.00$ ppm) or toluene ($\delta = 20.39$ ppm), and ^{119}Sn-external tetramethylstannane ($\delta = 0.00$ ppm). Chemical shift data are provided in ppm, with coupling constants in Hz. Abbreviations used are follows: s = singlet; d = doublet; t = triplet; h = heptet; m = complex multiplet.

Solid state ^{119}Sn spectra were recorded on a Bruker DSX 200 spectrometer equipped with a double-bearing CP/MAS probe at room temperature. The ^{119}Sn Hartmann−Hahn cross-polarization match was set with tetracyclohexyl tin using a ^{1}H 90° pulse of 4 μs. RAMP/CP/MAS (ramped/cross-polarization/magic angle spinning) experiments were used with a repetition delay of 10 s and the contact time was set at 2 ms. In each case, at least two spinning rates (4.5−9 kHz) were used to identify the isotropic chemical shift. The number of scans varied between 200 and 4000. For sample **2**, the repetition delay was set up at 30 s, as the ^{1}H T_1 relaxation time was extremely long. Such a long relaxation delay indicates very slow internal molecular motion resulting from arrangement of molecules in the crystal cell. The ^{119}Sn chemical shifts were calibrated indirectly using tetracyclohexyl tin ($\delta = -97.35$ ppm). The ^{119}Sn NMR chemical shift was allocated approximately to the center of gravity of the signal.

In the mass spectrometry, the positive-ion electrospray ionization (ESI) mass spectra were measured on an Esquire3000 ion trap analyzer (Bruker Daltonics, Bremen, Germany) in the range *m*/*z* 100−1000, and negative-ion ESI mass spectra were measured on the Platform quadrupole analyzer (Micromass, UK) in the range *m*/*z* 15−600. The ion trap was tuned to give an optimum response for *m*/*z* 500. The samples were dissolved in acetonitrile and analyzed by direct infusion at a flow rate of 1−3 μL/min. The selected precursor ions were further analyzed by MS/MS analysis with an ion trap analyzer under the following conditions: isolation width *m*/*z* = 8, ion source temperature 300 °C, flow rate and nitrogen pressure 4 L/min and 10 psi. Two mechanisms are involved in the ionization process of organotin compounds under ESI conditions. Similarly to recently published results,[18] the main process of the ion formation is the cleavage of the most labile bond, i.e., AB → $[A]^+ + [B]^-$. If the Sn−Cl bond is present in the structure, then this bond is cleaved first, yielding two complementary ions, $[M - Cl]^+$ and $[Cl]^-$. The cationic part of the molecule $[M - Cl]^+$ is mostly the base peak of the positive-ion ESI-MS and can be further studied by MS/MS analysis. The anionic part, $[Cl]^-$, is measured in the negative-ion mode. For negative ions with *m*/*z* lower than about 60, the quadrupole analyzer has to be used instead of the ion trap for their detection (e.g., $[Cl]^-$ at *m*/*z* 35 and 37). When the Sn−Cl bond is missing in the structure (**1**, **5**, and **9**), then the primary cleavage is Sn−phenyl and the cationization with alkali metal ions as a competitive ionization process can also occur. The formation of adducts $[M + Na]^+$ and $[M + K]^+$ is observed in most cases (the only process for **9**), but the relative abundances of these adducts are usually 1 order of magnitude lower than $[R_3Sn]^+$ ions. The adduct abundances depend on the amount of salts in the samples and solvents used for their analysis. Two compounds in our series contain three chlorine atoms (**4** and **8**) and both show unusual behavior during the analysis in the ion trap. They react in the mass spectrometer according to the equation M + M → M* (= 2M − $SnCl_4$) + $SnCl_4$. All identified ions in the spectra come from these condensed molecules except for the ion $[M - Cl]^+$ for **4** with the relative abundance 3% (see Experimental Section). The probable explanation for

(18) Růžička, A.; Dostál, L.; Jambor, R.; Buchta, V.; Brus, J.; Císařová, I.; Holčapek, M.; Holeček, J. *Appl. Organomet. Chem.* **2002**, *16*, 315.

this phenomenon is a long reaction time in the ion trap analyzer (in the range of milliseconds) compared to other mass analyzers.

Compound Preparation. Starting materials 1-bromo-2,6-bis(bromomethyl)benzene,[19] 1-bromo-2,6-bis(methoxymethyl)-benzene (L^1Br),[19] and 1-bromo-2,6-bis(isopropoxymethyl)-benzene (L^2Br)[20] were prepared analogously to the literature procedures. The compounds L^1Li and L^2Li were prepared in situ (see below).

Synthesis of 1-Bromo-2,6-bis(*tert*-butoxymethyl)benzene (L^3Br). A solution of 1-bromo-2,6-bis(bromomethyl)-benzene in 20 mL of benzene (3.11 g, 9.07 mmol) was added to the stirred suspension of potassium *tert*-butoxide (3.04 g, 27.2 mmol) in 30 mL of benzene; the solution was stirred for a further 2 h. This solution was hydrolyzed by 10 mL of water, and the aqueous phase was washed with 20 mL of benzene. Benzene extracts were combined and dried over anhydrous sodium sulfate. The yellowish solution was filtered, the benzene filtrate was evaporated, and a pale yellow oil remained, which was distilled to give 1.7 g (57.4%) of L^3Br as a colorless oil, bp 95−100 °C/20 Pa. Anal. Calcd for $C_{16}H_{25}BrO_2$ (MW 329.29): C, 58.36; H, 7.65. Found: C, 58.16; H, 7.44. ^{1}H NMR ($CDCl_3$, 360 MHz): δ (ppm) 1.31 (s, 18H, CH_3), 4.51 (s, 4H, CH_2), 7.30 (t, 1H, Ar-H), 7.45 (d, 2H, Ar-H). ^{13}C NMR ($CDCl_3$, 90 MHz): δ (ppm) 27.6 (*C*H$_3$), 63.8 (*C*H$_2$), 73.6 (O*C*Me$_3$), C_6H_3 (not assigned) 121.9, 126.9, 127.3, 139.4.

Synthesis of 2,6-Bis(*tert*-butoxymethyl)phenyllithium (L^3Li). A 1.1 mL sample of *n*-BuLi (2.008 M) was added to the stirred solution of L^3Br (0.66 g, 2 mmol) in 10 mL of hexane at ambient temperature; the solution was stirred for a further 1 h. The solution was concentrated to 5 mL and left to crystallize overnight. The white solid was filtrated at −78 °C and washed with 3 mL of precooled pentane to give pure L^3Li in 89% yield. ^{1}H NMR (toluene-d_8, 360 MHz): δ (ppm) 1.15 (s, 18H, CH_3), 4.29 (s, 4H, CH_2), 7.18 (m, 3H, Ar-H).

Synthesis of Ph_3SnL^1 (1). A 3.3 mL portion of *n*-BuLi (2.008 M) was added to the stirred solution of L^1Br (1.47 g, 5.98 mmol) in 15 mL of Et_2O at −78 °C; the solution was stirred for a further 2 h at this temperature, followed by dropwise addition to a precooled (−78 °C) 20 mL suspension of hexane containing 2.2 g (5.68 mmol) of Ph_3SnCl. After addition, the solution faded to pale yellow. The mixture was stirred for a further 2 h, and then the solvent was evaporated in vacuo and the residue was dissolved in $CHCl_3$. After the resulting solid was filtered off, the $CHCl_3$ filtrate was concentrated, layered with pentane, and left to crystallize to **1**, which was obtained as a white solid. Yield: 2.1 g (68%), mp 87−95 °C. Anal. Calcd for $C_{28}H_{28}O_2Sn$ (MW 515.21): C, 65.27; H, 5.48. Found: C, 67.01; H, 5.14. MW = 516. MS: *m*/*z* 477, 9%, $[M + K - C_6H_6]^+$; *m*/*z* 461, 11%, $[M + Na - C_6H_6]^+$; *m*/*z* 439, 100%, $[M - C_6H_5]^+$. MS/MS of 439 (collision amplitude 1 V): *m*/*z* 407, 10%, $[M - C_6H_5 - CH_3OH]^+$; *m*/*z* 377, 95%, $[M - C_6H_5 - CH_3OH - CH_2O]^+$; *m*/*z* 375, 100%, $[M - C_6H_5 - 2 \times CH_3OH]^+$; *m*/*z* 347, 15%, $[M - C_6H_5 - 2 \times CH_3OCH_3]^+$; *m*/*z* 299, 4%, $[M - C_6H_5 - CH_3OH - CH_2O - C_6H_6]^+$; *m*/*z* 255, 22%, $[M - C_6H_5 - 2 \times CH_3OH - Sn]^+$; *m*/*z* 197, 7%, $[C_6H_5Sn]^+$; *m*/*z* 179, 6%, $[M - C_6H_5 - 2 \times CH_3OH - Sn - C_6H_4]^+$; *m*/*z* 165, 4%, $[C_6H_3(CH_2OCH_3)_2]^+$. ^{1}H NMR ($CDCl_3$, 360 MHz): δ (ppm) 2.69 (s, 6H, CH_3), 4.16 (s, 4H, CH_2, $^nJ(^{119}Sn,^1H) = 5.1$ Hz), 7.23−7.65 (complex pattern, 18H, $SnPh_3$, SnC_6H_3). ^{13}C NMR ($CDCl_3$, 90 MHz): δ (ppm) 57.0 (*C*H$_3$), 75.4 (*C*H$_2$), SnC_6H_3, 137.2 (C(1), $^1J(^{119}Sn,^{13}C) = 570.8$ Hz), 128.0, 128.7, 146.9; $SnPh_3$, 142.4 (C(1′), $^1J(^{119}Sn,^{13}C) = 543.1$ Hz), 127.9, 128.1, 136.8.

Synthesis of Ph_2ClSnL^1 (2), $PhCl_2SnL^1$ (3), and Cl_3SnL^1 (4). A procedure similar to that for **1** was followed. The precooled (−78 °C) 20 mL suspension of hexane contained 1.95 g (5.68 mmol) of Ph_2SnCl_2, 1.72 g (5.68 mmol) of $PhSnCl_3$, and 1.48 g (5.68 mmol) of $SnCl_4$.

Compound 2. Yield: 2.3 g (81%), mp 185−190 °C. Anal. Calcd for $C_{22}H_{23}ClO_2Sn$ (MW 473.56): C, 55.80; H, 4.90. Found: C, 55.50; H, 4.75. MW = 474. MS: *m*/*z* 513, 3%, $[M + K]^+$; *m*/*z* 497, 3%, $[M + Na]^+$; *m*/*z* 439, 100%, $[M - Cl]^+$. ^{1}H NMR ($CDCl_3$, 360 MHz): δ (ppm) 2.96 (s, 6H, CH_3), 4.54 (s, 4H, CH_2, $^nJ(^{119}Sn,^1H = 7.9$ Hz)), 7.20−7.75 (complex pattern, 13H, $SnPh_2$, SnC_6H_3). ^{13}C NMR ($CDCl_3$, 90 MHz): δ (ppm) 57.6 (*C*H$_3$), 74.1 (*C*H$_2$), SnC_6H_3, 135.3 (C(1), $^1J(^{119}Sn,^{13}C) = 729.6$ Hz), 126.8, 129.1, 146.0; $SnPh_2$, 142.4 (C′(1), $^1J(^{119}Sn,^{13}C) = 733.9$ Hz), 128.4, 128.9, 135.4.

Compound 3. Yield: 2.4 g (92%), mp 188−192 °C. Anal. Calcd for $C_{16}H_{18}Cl_2O_2Sn$ (MW 431.91): C, 44.49; H, 4.20. Found: C, 44.10; H, 4.20. MW = 432. MS: *m*/*z* 471, 12%, $[M + K]^+$; *m*/*z* 455, 20%, $[M + Na]^+$; *m*/*z* 397, 100%, $[M - Cl]^+$. ^{1}H NMR ($CDCl_3$, 360 MHz): δ (ppm) 3.17 (s, 6H, CH_3), 4.68 (s, 4H, CH_2, $^nJ(^{119}Sn,^1H) = 10.8$ Hz), 7.18−7.81 (complex pattern, 8H, SnPh, SnC_6H_3). ^{13}C NMR ($CDCl_3$, 90 MHz): δ (ppm) 57.9 (*C*H$_3$), 73.1 (*C*H$_2$), SnC_6H_3, 134.7 (C(1), $^1J(^{119}Sn,^{13}C) = 997.4$ Hz), 126.3, 130.2, 144.9; SnPh, 141.1 (C′(1), $^1J(^{119}Sn,^{13}C) = 1027.2$ Hz), 129.2, 130.6, 134.7.

Compound 4. Yield: 1.1 g (47%), mp 75−80 °C. Anal. Calcd for $C_{10}H_{13}Cl_3O_2Sn$ (MW 390.26): C, 30.78; H, 3.36. Found: C, 30.48; H, 3,05. MW = 390. MW* = 2 × M − $SnCl_4$ = 520. MS: *m*/*z* 485, 100%, $[M^* - Cl]^+$; *m*/*z* 455, 8%, $[M^* - Cl - CH_2O]^+$; *m*/*z* 355, 3%, $[M - Cl]^+$. MS/MS of 485 (collision amplitude 1 V): *m*/*z* 455, 94%, $[M^* - Cl - CH_2O]^+$; *m*/*z* 425, 33%, $[M^* - Cl - 2 \times CH_2O]^+$; *m*/*z* 395, 8%, $[M^* - Cl - 3 \times CH_2O]^+$; *m*/*z* 365, 8%, $[M^* - Cl - 4 \times CH_2O]^+$; *m*/*z* 349, 8%, $[M^* - Cl - 3 \times CH_2O - CH_3OCH_3]^+$; *m*/*z* 285, 19%, $[C_6H_3(CH_2OCH_3)_2Sn]^+$; *m*/*z* 255, 7%, $[285 - CH_2O]^+$; *m*/*z* 223, 8%, $[285 - CH_2O - CH_3OH]^+$; *m*/*z* 205, 100%, $[CH_3SnCl_2]^{\bullet+}$; *m*/*z* 192, 85%, $[H_2SnCl_2]^{\bullet+}$. ^{1}H NMR ($CDCl_3$, 360 MHz): δ (ppm) 3.58 (s, 6H, CH_3), 4.68 (s, 4H, CH_2, $^nJ(^{119}Sn,^1H) = 12.35$ Hz), 7.23 (d, 2H, SnC_6H_3), 7.43 (t, 1H, SnC_6H_3). ^{13}C NMR ($CDCl_3$, 90 MHz): δ (ppm) 56.9 (*C*H$_3$), 73.6 (*C*H$_2$), SnC_6H_3, 133.3 (C(1), $^1J(^{119}Sn,^{13}C) = 1372.2$ Hz), 125.7, 129.9, 142.9.

Synthesis of Ph_3SnL^2 (5). A 2.76 mL sample of *n*-BuLi (2.008 M) was added to the stirred solution of L^2Br (1.67 g, 5.54 mmol) in 15 mL of hexane at RT; the solution was stirred for a further 3 h at this temperature, followed by dropwise addition to a 10 mL suspension of hexane containing 2.03 g (5.27 mmol) of Ph_3SnCl. After addition, the solution faded to pale yellow. The mixture was stirred for a further 5 h, and then the solvent was evaporated in vacuo and the residue was dissolved in $CHCl_3$. After the resulting solid was filtered off, the $CHCl_3$ filtrate was concentrated, layered with pentane, and left to crystallize to **5**, which was obtained as a white solid. Yield: 2.2 g (70%). Anal. Calcd for $C_{32}H_{36}O_2Sn$ (MW 571.32): C, 67.27; H, 6.35. Found: C, 66.91; H, 6.14. MW = 572. MS: *m*/*z* 495, 100%, $[M - C_6H_5]^+$; *m*/*z* 453, 7%, $[M - C_6H_5 - propene]^+$. MS/MS of 495 (collision amplitude 0.9 V): *m*/*z* 453, 100%, $[M - C_6H_5 - propene]^+$; *m*/*z* 411, 15%, $[M - C_6H_5 - 2 \times propene]^+$; *m*/*z* 393, 11%, $[M - C_6H_5 - propene - 2\text{-propanol}]^+$; *m*/*z* 351, 23%, $[(C_6H_6)_3Sn]^+$; *m*/*z* 315, 45%, $[M - C_6H_5 - C_6H_6 - propene - 2\text{-propanol}]^+$; *m*/*z* 179, 39%, $[C_6H_3C_6H_3\text{-}CH_3(CH_2)]^+$. ^{1}H NMR ($CDCl_3$, 360 MHz): δ (ppm) 0.85 (d, 12H, CH_3), 3.14 (h, 2H, OCH), 4.34 (s, 4H, CH_2, $^nJ(^{119}Sn,^1H) = 6.6$ Hz), 7.27−7.68 (complex pattern, 18H, $SnPh_3$, SnC_6H_3). ^{13}C NMR ($CDCl_3$, 90 MHz): δ (ppm) 22.1 (*C*H$_3$), 70.7 (OCH) 71.9 (*C*H$_2$), SnC_6H_3, 135.5 (C(1), $^1J(^{119}Sn,^{13}C) = 542.4$ Hz), 127.2, 129.4, 147.3; $SnPh_3$, 141.5 (C′(1), $^1J(^{119}Sn,^{13}C) = 527.1$ Hz), 128.3, 128.6, 136.8.

Synthesis of Ph_2ClSnL^2 (6), $PhCl_2SnL^2$ (7), and Cl_3SnL^2 (8). A procedure similar to that for **5** was followed. The 10 mL suspension of hexane contained 1.81 g (5.26 mmol) of Ph_2SnCl_2, 1.59 g (5.26 mmol) of $PhSnCl_3$, and 1.37 g (5.26 mmol) of $SnCl_4$.

Compound 6. Yield: 2.5 g (85%), mp 65−70 °C. Anal. Calcd for $C_{26}H_{31}ClO_2Sn$ (MW 529.67): C, 58.96; H, 5.90. Found: C,

(19) Markies, P. R.; Altink R. M.; Villena A.; Akkerman O. S.; Bickelhaupt F.; Smeets W. J. J.; Spek A. L. *J. Organomet. Chem.* **1991**, *402*, 289.

(20) Ortiz, B.; Walls, F.; Barrios, H.; Obregon, S. R.; Pinelo, L. *Synth. Commun.* **1993**, *6*, 749.

58.60; H, 5.60. MW = 530. MS: *m/z* 495, 100%, $[M - Cl]^+$; *m/z* 453, 4%, $[M - Cl - propene]^+$. MS/MS of 495 (collision amplitude 1 V): *m/z* 453, 100%, $[M - Cl - propene]^+$; *m/z* 411, 22%, $[M - Cl - 2 \times propene]^+$; *m/z* 393, 8%, $[M - Cl - propene - 2\text{-propanol}]^+$; *m/z* 351, 18%, $[(C_6H_5)_3Sn]^+$; *m/z* 315, 55%, $[M - Cl - C_6H_6 - propene - 2\text{-propanol}]^+$; *m/z* 239, 8%, $[M - Cl - C_6H_6 - propene - 2\text{-propanol} - C_6H_4]^+$; *m/z* 195, 3%, $[M - Cl - C_6H_6 - propene - 2\text{-propanol} - Sn]^+$; *m/z* 179, 25%, $[HOCH_2C_6H_3CH_2OCH(CH_3)_2]^+$. ^{1}H NMR ($CDCl_3$, 360 MHz): δ (ppm) 0.80 (d, 12H, CH_3), 3.53 (h, 2H, OCH), 4.63 (s, 4H, CH_2), 7.24−7.75 (complex pattern, 13H, $SnPh_2$, SnC_6H_3). ^{13}C NMR ($CDCl_3$, 90 MHz): δ (ppm) 21.1 (*C*H_3), 71.9 (O*C*H) 69.3 (*C*H_2), SnC_6H_3, 134.2 (C(1), $^1J(^{119}Sn,^{13}C) = 683.8$ Hz), 127.1, 129.6, 146.9; $SnPh_2$, 143.2 (C′(1), $^1J(^{119}Sn,^{13}C) = 737.9$ Hz), 128.4, 129.2, 135.6.

Compound 7. Yield: 2.4 g (90%), mp 135−137 °C. Anal. Calcd for $C_{20}H_{26}Cl_2O_2Sn$ (MW 488.02): C, 49.22; H, 5.37. Found: C, 48.92; H, 5.20. MW = 488. MS: *m/z* 527, 23%, $[M + K]^+$; *m/z* 511, 6%, $[M + Na]^+$; *m/z* 453, 100%, $[M - Cl]^+$; *m/z* 411, 3%, $[M - Cl - propene]^+$. ^{1}H NMR ($CDCl_3$, 360 MHz): δ (ppm) 0.89 (d, 12H, CH_3), 3.75 (h, 2H, OCH), 4.72 (s, 4H, CH_2, $^nJ(^{119}Sn,^1H = 9.1$ Hz)), 7.20−7.80 (complex pattern, 8H, SnPh, SnC_6H_3). ^{13}C NMR ($CDCl_3$, 90 MHz): δ (ppm) 21.3 (*C*H_3), 73.0 (O*C*H) 67.8 (*C*H_2), SnC_6H_3, 132.9 (C(1), $^1J(^{119}Sn,^{13}C) = 930.5$ Hz), 127.1, 130.8, 146.1; SnPh, 143.4 (C′(1), $^1J(^{119}Sn,^{13}C) = 996.1$ Hz), 128.9, 130.4, 135.4.

Compound 8. Yield: 0.9 g (39%), mp 68−72 °C. Anal. Calcd for $C_{14}H_{21}Cl_3O_2Sn$ (MW 446.36): C, 37.67; H, 4.74. Found: C, 37.97; H, 4.95. MW = 446. MW* = 2 × M − $SnCl_4$ = 632. MS: *m/z* 655, 3%, $[M^* + Na]^+$; *m/z* 597, 100%, $[M^* - Cl]^+$; *m/z* 519, 10%, $[M^* - Cl - HCl - propene]^+$; *m/z* 477, 1%, $[M^* - Cl - HCl - 2 \times propene]^+$. MS/MS of 597 (collision amplitude 0.6 V): *m/z* 519, 100%, $[M^* - Cl - HCl - propene]^+$; *m/z* 477, 50%, $[M^* - Cl - HCl - 2 \times propene]^+$; *m/z* 435, 32%, $[M^* - Cl - HCl - 3 \times propene]^+$; *m/z* 393, 20%, $[M^* - Cl - HCl - 4 \times propene]^+$; *m/z* 375, 7%, $[M^* - Cl - HCl - 4 \times propene - H_2O]^+$. ^{1}H NMR ($CDCl_3$, 360 MHz): δ (ppm) 1.34 (d, 12H, CH_3), 4.32 (h, 2H, OCH), 4.73 (s, 4H, CH_2, $^nJ(^{119}Sn,^1H) = 11.1$ Hz), 7.25 (d, 2H, SnC_6H_3), 7.42 (t, 1H, SnC_6H_3). ^{13}C NMR ($CDCl_3$, 90 MHz): δ (ppm) 21.7 (*C*H_3), 72.4 (O*C*H) 69.7 (*C*H_2), SnC_6H_3, 139.6 (C(1), $^1J(^{119}Sn,^{13}C) = 1036.2$ Hz), 126.9, 130.0, 145.3.

Synthesis of Ph_3SnL^3 (9). A 1.2 g (4.7 mmol) portion of L^3Li in hexane was added dropwise to a stirred suspension of 1.8 g (4.7 mmol) of Ph_3SnCl in 10 mL of hexane. After addition, the solution was heated for 5 h at 60 °C and then stirred overnight. Then the solvent was evaporated in vacuo and the residue was dissolved in $CHCl_3$. After the resulting solid was filtered off, the $CHCl_3$ filtrate was concentrated, covered with pentane, and left to crystallize to **9**, which was obtained as a white solid. Yield: 2.67 g (95%), mp 155−157 °C. Anal. Calcd for $C_{34}H_{40}O_2Sn$ (MW 599.38): C, 68.13; H, 6.73. Found: C, 67.91; H, 6.51. MW = 600. MS: *m/z* 639, 70%, $[M + K]^+$; *m/z* 623, 100%, $[M + Na]^+$. ^{1}H NMR ($CDCl_3$, 360 MHz): δ (ppm) 0.96 (s, 18H, CH_3), 4.39 (s, 4H, CH_2, $^nJ(^{119}Sn,^1H) = 7.7$ Hz), 7.41−7.78 (complex pattern, 18H, $SnPh_3$, SnC_6H_3). ^{13}C NMR ($CDCl_3$, 90 MHz): δ (ppm) 27.2 (*C*H_3), 67.0 (*C*H_2), 73.4 (O*C*Me_3), SnC_6H_3, 133.6 (C(1), $^1J(^{119}Sn,^{13}C = 536.1$ Hz), 125.9, 129.7, 147.9; $SnPh_3$, 141.4 (C′(1), $^1J(^{119}Sn,^{13}C = 520.9$ Hz), 128.5, 128.7, 136.8.

Synthesis of Ph_2ClSnL^3 (10) and $PhCl_2SnL^3$ (11). A procedure similar to that in **9** was followed, without the heating, and the solutions were stirred for only 3 h, after the Li salt was added into the hexane solution. The 10 mL suspension of hexane contained 2.4 g (7 mmol) of Ph_2SnCl_2 and 1.27 g (4.2 mmol) of $PhSnCl_3$.

Compound 10. Yield: 3.52 g (90%), mp 118−123 °C. Anal. Calcd for $C_{28}H_{35}ClO_2Sn$ (MW 557.72): C, 60.30; H, 6.33. Found: C, 60.55; H, 6.62. MW = 558. MS: *m/z* 523, 100%, $[M - Cl]^+$; *m/z* 495, 2%, $[M - Cl - ethene]^+$; *m/z* 467, 15%, $[M - Cl - isobutene]^+$; *m/z* 411, 10%, $[M - Cl - 2 \times isobutene]^+$. ^{1}H NMR ($CDCl_3$, 360 MHz): δ (ppm) 0.94 (s, 18H, CH_3), 4.62 (s, 4H, CH_2,), 7.27−7.80 (complex pattern, 15H, $SnPh_2$, SnC_6H_3). ^{13}C NMR ($CDCl_3$, 90 MHz): δ (ppm) 27.4 (*C*H_3), 65.7 (*C*H_2), 75.6 (O*C*Me_3), SnC_6H_3, 134.2 (C(1), $^1J(^{119}Sn,^{13}C) = 714.4$ Hz), 126.4, 129.8, 147.8; $SnPh_2$, 143.3 (C′(1), $^1J(^{119}Sn,^{13}C) = 720.6$ Hz), 128.5, 129.3, 135.6.

Compound 11. Yield: 2.02 g (93%), mp 112−115 °C. Anal. Calcd for $C_{22}H_{30}Cl_2O_2Sn$ (MW 516.07): C, 51.20; H, 5.86. Found: C, 51.55; H, 6.12. MW = 516. MS: *m/z* 555, 15%, $[M + K]^+$; *m/z* 539, 32%, $[M + Na]^+$; *m/z* 519, 7%, $[M + K - HCl]^+$; *m/z* 503, 6%, $[M + Na - HCl]^+$; *m/z* 481, 100%, $[M - Cl]^+$; *m/z* 425, 54%, $[M - Cl - isobutene]^+$; *m/z* 369, 58%, $[M - 2 \times isobutene]^+$. ^{1}H NMR ($CDCl_3$, 360 MHz): δ (ppm) 0.98 (s, 18H, CH_3), 4.69 (s, 4H, CH_2, $^nJ(^{119}Sn,^1H) = 8.8$ Hz), 7.16−7.72 (complex pattern, 8H, SnPh, SnC_6H_3). ^{13}C NMR ($CDCl_3$, 90 MHz): δ (ppm) 27.3 (*C*H_3), 64.6 (*C*H_2), 77.7 (O*C*Me_3), SnC_6H_3, 132.1 (C(1), $^1J(^{119}Sn,^{13}C) = 872.4$ Hz), 127.1, 130.6, 146.8; SnPh, 144.6 (C′(1), $^1J(^{119}Sn,^{13}C) = 945.9$ Hz), 128.6, 130.6, 135.3.

Attempt to Prepare Cl_3SnL^3. All attempts to prepare this compound result only in a mixture of unseparable products. The NMR tube experiment at 200 K revealed no reaction during 20 min after the addition of $SnCl_4$ (132 mg, 0.5 mmol) to the toluene solution of L^3Li (130 mg, 0.5 mmol). After this period, the NMR tube was allowed to warm to 260 K and the reaction proceeded, resulting in the same mixture of products. The GC−MS analysis of the vapor over the sample solution indicated the presence of di(*tert*-butyl) ether, *tert*-butylmethyl ether, *tert*-butyl acetate, and benzene. The precipitating nonsoluble solid was identified as LiCl.

Crystallography. Crystals suitable for X-ray structure determination were obtained by vapor diffusion of *n*-hexane into the 5% dichloromethane solution for compounds **1**, **2**, **3**, **4**, and **7**, respectively, and by crystallization of **11** from chloroform solution. Data for all the colorless crystals were collected at 150(2) K on a Nonius KappaCCD diffractometer using Mo Kα radiation ($\lambda = 0.71073$ Å), with a graphite monochromator. The structures were solved by direct methods (SIR92). All reflections were used in the structure refinement based on F^2 by the full-matrix least-squares technique (SHELXL97). The hydrogen atoms were mostly localized on a difference Fourier map; however, to ensure uniformity of treatment of all crystals, all the hydrogens were recalculated into idealized positions (riding model) and assigned temperature factors $H_{iso}(H) = 1.2U_{eq}$(pivot atom) or $1.5U_{eq}$ for the methyl moiety. Absorption corrections were carried out using the multiscan procedure (SORTAV). It follows from the last cycle of refinement of all the structures that $(\Delta/\delta)_{max} < 0.003$. Crystallographic data for individual structures are summarized in Table 1. A full list of crystallographic data and parameters including fractional coordinates are deposited under CCDC 183103 (**1**), 183104 (**2**), 183105 (**3**), 183106 (**4**), 183107 (**7**), and 183108 (**11**), at the Cambridge Crystallographic Data Center, 12 Union Road, Cambridge, CB2 1EZ, UK [Fax: int. code + 44(1223)336-033; E-mail: deposit@ccdc.cam.ac.uk].

Acknowledgment. The authors wish to thank the Grant Agency of the Czech Republic (grants nos. 203/00/0920, 203/99/M037) and The Ministry of Education of the Czech Republic (LN00A028 project) for financial support.

Supporting Information Available: Tables of all crystal data and structure refinement, atomic coordinates, anisotropic displacement parameteres, and geometric data for compounds **1**−**4**, **7**, and **11**. This material is available free of charge via the Internet at http://pubs.acs.org.

OM020361I